# Mechanistic Assessment of Droplet-Size-Dependent Spray Thermal Effectiveness for APR Containment Using CAP 3.1

*Yong -Ju Cho[a*], Sun-Hong Yoon[a], Jae-Yul Kim[b]*
*[a]KEPCO-E&C, Nuclear Technology Research Dept, 269 Hyeoksin-ro, Gimcheon-si, 39660*
*[b]KEPCO-E&C, Nuclear Engineering Dept, 269 Hyeoksin-ro, Gimcheon-si, 39660*
*[*]Corresponding author: cyongju93@kepco-enc.com*

***Keywords : Containment Spray, Thermal Effectiveness, Droplet Size, CAP 3.1, Three-Field Model, APR1400.**

## 1.Introduction

The containment building is designed to maintain structural integrity during postulated accidents by accommodating thermodynamic loads generated from mass and energy release into the containment atmosphere. Accurate prediction of containment pressure and temperature (P/T) transients is therefore essential for safety demonstration, since peak and long-term responses provide direct margins to containment design limits. In licensing practice, such analyses must be technically rigorous, traceable, and regulatorily defensible.

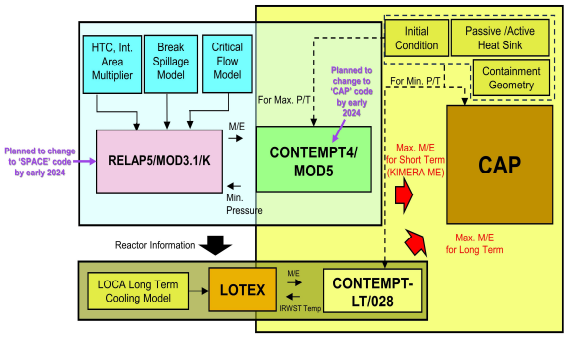


Fig. 1. Schematic of APR Containment Pressure and Temperature Analysis[1]

As nuclear power plant designs have advanced, containment thermal–hydraulic behavior has become increasingly governed by coupled multi-phase processes, including condensation, evaporation, and droplet heat transfer. Containment spray performance is strongly dependent on droplet–atmosphere interaction, making spray characterization a licensing-relevant modeling input rather than a simple numerical parameter.

The adoption of CAP introduces a structural change in the containment P/T analysis methodology. As shown in Fig. 1, the conventional framework combined system thermal–hydraulic codes for mass and energy release calculations with CONTEMPT-LT/028 for containment response evaluation. In contrast, the CAP-based methodology employs a three-field formulation consisting of gas, continuous liquid, and dispersed droplet phases [1]. This mechanistic framework enables direct resolution of droplet–gas interfacial heat and mass transfer within the containment response model. Therefore, the transition to CAP represents not merely a code replacement but an evolution of the containment P/T methodology, particularly in the treatment of spray heat transfer.

ANSI/ANS-56.5 requires detailed droplet size characterization for credited spray nozzles, including statistically meaningful droplet diameter spectra with increments of 100 μm or less [2]. These requirements emphasize the need to evaluate spray thermal performance explicitly as a function of droplet size and to establish a technically traceable modeling basis.

Previous spray evaluations were commonly performed using CONSPRAY-based correlations, where spray efficiency was inferred indirectly from assumed droplet behavior and residence time. In contrast, the present study employs CAP 3.1 to directly compute spray thermal effectiveness using a mechanistic three-field model. After preliminary parameter bounding with CONSPRAY, a structured droplet diameter sensitivity analysis is conducted to quantify spray thermal effectiveness as a function of droplet size. This approach provides a regulatorily defensible basis for determining spray efficiency in APR containment P/T analysis.

## 2. Methods and Node Schematic

### *2.1 Criteria*

The present methodology follows a licensing-oriented interpretation of U.S. consensus standards governing containment spray characterization and containment P/T transient analysis. Two standards form the primary regulatory basis of this study.

ANSI/ANS-56.5 identifies droplet size distribution as a key parameter influencing spray performance and requires detailed characterization of the droplet diameter spectrum for credited spray nozzles. The standard specifies statistically meaningful droplet size data with diameter increments of 100 μm or less, together with documentation of data sources and associated uncertainties [2]. Consistent with this requirement, the present study treats droplet diameter as an explicit sensitivity parameter and performs a systematic diameter sweep to quantify its impact on spray thermal effectiveness within a traceable parameter space.

ANSI/ANS-56.4 provides criteria for containment P/T transient analysis and addresses the representation of spray effects in the vapor region. The standard links spray efficiency evaluation to ANSI/ANS-56.5 and allows simplified modeling assumptions depending on

thermodynamic conditions, including neglecting detailed droplet residence effects in highly simplified analyses [3]. It also provides guidance on treatment of evaporation and drainage to the sump under saturated or superheated conditions.

In contrast to such simplifications, the present work employs the mechanistic three-field capability of CAP to explicitly model dispersed droplets and compute droplet thermal response as a function of diameter and effective fall height. This approach enhances traceability and provides a defensible technical basis when spray thermal effectiveness is credited in containment P/T evaluations.

### *2.2 Node Schematic*

Figure 2 illustrates the node schematic adopted for the CAP 3.1-based spray thermal performance evaluation. The containment is modeled as a single, well-mixed control volume to isolate droplet–atmosphere heat and mass transfer effects within a controlled parameter space. The containment free volume is fixed at 1.86E+6 ft³ with a cell height of 100 ft, which is also defined as the effective spray fall height (droplet residence path).

The initial atmosphere temperature is set to 130 °F with 100% relative humidity. Spray water is supplied at 50 °F with a constant flow rate of 5,000 gpm (≈ 695 lbm/s). To avoid non-physical initialization effects, the initial droplet temperature is set equal to the spray inlet temperature.

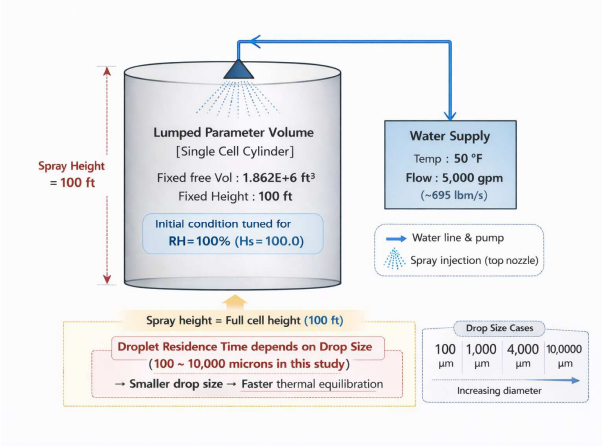


Fig. 2. Node Schematic for CAP Spray Thermal Performance Evaluation

Droplet diameter is treated as a parametric variable, and representative diameters ranging from 100 µm to 10,000 µm are evaluated to quantify droplet-size effects. Smaller droplets are expected to approach thermal equilibrium more rapidly due to enhanced surface-area-to-volume ratio under identical fall height conditions.

Based on the design-basis accident conditions of Shin-Kori Units 3 and 4 (Saeul Units 3 and 4), a parametric study is performed to determine a conservative minimum bounding value of containment spray thermal effectiveness for LOCA and MSLB scenarios.

In LOCA, containment behavior is governed by sustained mass and energy release followed by condensation and heat removal. In MSLB, steam release dominates the early phase, but operator action is assumed to terminate the break-driven discharge after 30 minutes. Consequently, spray performance must remain acceptable not only during the initial release period but also during the post-release phase, when containment response is controlled by residual vapor inventory and heat structures.

From the present evaluation, the spray thermal effectiveness is calculated as 100% under the bounding conditions. Therefore, containment spray thermal effectiveness of 100% is considered acceptable as the minimum bound for containment P/T analysis throughout the entire postulated accident duration.

### *2.3 Containment Spray Heat Transfer Mode*

Containment spray removes energy from the atmosphere through coupled heat and mass transfer between the gas mixture (steam and non-condensable gas) and dispersed droplets. In conventional CAP applications, spray heat transfer has often been represented using a thermal-equilibrium model requiring user-defined spray efficiency. While convenient for P/T calculations, this approach relies on prescribed efficiency values and may become inconsistent when droplet residence time is insufficient for full thermal equilibration, particularly in multi-compartment nodalization [4].

(1) Steam contribution (energy change of steam)

$$\frac{q_s}{A_i} = -\left(\frac{P_s}{P_t}\right) h_{conv,s}(T_g - T_i) - \Gamma_{hg,sat}$$

(2) Non-condensable contribution (energy change of non-condensable gas)

$$\frac{q_{nc}}{A_i} = -\left(\frac{P_{nc}}{P_t}\right) h_{conv,nc}(T_g - T_d)$$

(3) Droplet contribution (energy change of droplet)

$$\frac{q_d}{A_i} = h_{conv,d}(Ti - Td) + \Gamma_{hf,sat} + \left(\frac{P_{nc}}{P_t}\right) h_{conv,nc}(Tg - Td)$$

where $q_s, q_{nc}$ and $q_d$ are the energy change rates of steam, non-condensable gas, and droplet, respectively; $A_i$ is interfacial area; $P_t$ is total pressure; $P_s$ and $P_{nc}$ are steam and non-condensable partial pressures; $T_g$ is bulk gas temperature; $T_d$ is bulk droplet temperature; $T_i$ is interfacial temperature; and Γ is interfacial mass transfer rate .

The gas-side convective heat transfer coefficient is calculated in the Ranz–Marshall form for a moving droplet [5].

$$h_{conv,v} = (2.0 + 0.6Re^{\frac{1}{2}} \cdot pr^{\frac{1}{3}}) \cdot k_g/D_d$$

Here Re is Reynolds number, Pr is Prandtl number, $k_g$ is gas thermal conductivity, and $D_d$ is droplet size. The droplet-side heat transfer coefficient can further incorporate subcooling and phase-change related effects through an augmented correlation form [6].

This mechanistic formulation explicitly links spray heat transfer to droplet diameter (through $D_d$ and Re), gas properties ($k_g$, Pr), and the thermodynamic state (through $P_s / P_t$, $P_{nc} / P_t$ and Γ), thereby providing a transparent basis to evaluate how droplet size and residence path affect spray thermal performance without prescribing an priori efficiency.

## 3.Analysis Results

A total of 50 sensitivity cases were performed using CAP 3.1 to quantify the dependence of spray thermal effectiveness on droplet diameter. The droplet diameter varied from 100 μm to 10,000 μm in systematic increments, consistent with the intent of ANSI/ANS-56.5 regarding droplet size resolution. For each case, the containment atmosphere temperature, droplet temperature, relative humidity, and corresponding steady-state averaged spray thermal efficiency were evaluated.

The evaluation of spray performance requires determining the spray thermal effectiveness for each representative droplet size group. In the present study, spray thermal effectiveness, η, is defined as

$$\eta = \frac{T_d - T_{d,0}}{T_{sat} - T_{d,0}}$$

Where, $T_{sat}$ is the saturation temperature corresponding to the steam partial pressure, and $T_{d,0}$ is the initial droplet temperature at the spray inlet.

The initial containment conditions were defined according to the node schematic described in Section 2.2. The containment atmosphere was initialized at 130 °F with 100% relative humidity, while the spray inlet water temperature was fixed at 50 °F. The droplet temperature was initially set equal to the spray inlet temperature to avoid non-physical startup transients. A constant spray flow rate of 5,000 gpm was imposed for all sensitivity cases.

Figures 3 through 6 present the transient responses of the atmosphere temperature, droplet temperature, and relative humidity for representative droplet diameters. For small droplets (≤ 2,000 μm), the droplet temperature rapidly approaches the local saturation temperature corresponding to the steam partial pressure, indicating strong thermal coupling between the dispersed droplet phase and the gas phase. The relative humidity remains effectively at saturation, confirming that condensation on the droplet surface dominates the heat removal mechanism under the selected conditions.

For intermediate droplet sizes (approximately 2,450–3,100 μm), partial deviation from thermal equilibrium is observed. The droplet temperature does not fully reach the saturation temperature before reaching the sump, resulting in reduced interfacial heat and mass transfer effectiveness. This behavior directly reflects the increased droplet thermal inertia and reduced surface-area-to-volume ratio as droplet size increases.

For large droplets (≥ 4,000 μm), the droplet temperature remains significantly below the local saturation temperature throughout its residence time. As shown in Figure 7, the temperature difference between the saturation temperature and the droplet temperature persists over the falling path, indicating incomplete thermal equilibration. Consequently, the spray thermal effectiveness decreases substantially.

The steady-state average results are summarized in Table 1. For droplet diameters of 100 μm, 1,000 μm, and 2,000 μm, the spray thermal efficiency is calculated as 100%. In these cases, the droplet temperature converges to the saturation temperature within the available residence time, and the spray behaves effectively as a thermal-equilibrium sink.

Table 1. Results of Spray Thermal Effectiveness

| Size [μm] | Total Press [psi] | Steam Press [psi] | Droplet Temp [F] | Atoms Temp [F] | Thermal Efficiency [%] |
|---|---|---|---|---|---|
| 100 | 16.1 | 0.178 | 50.1 | 50.1 | 100 |
| 1000 | 16.1 | 0.179 | 50.1 | 50.1 | 100 |
| 2000 | 16.1 | 0.179 | 50.1 | 50.2 | 100 |
| 2450 | 16.1 | 0.179 | 50.1 | 50.3 | 87.8 |
| 3100 | 16.1 | 0.180 | 50.1 | 50.4 | 50.0 |
| 4000 | 16.1 | 0.180 | 50.1 | 50.5 | 33.3 |
| 10,000 | 16.1 | 0.184 | 50.1 | 51.4 | 11.1 |

Beyond 2,000 μm, efficiency begins to decrease. At 2,450 μm, the thermal efficiency is reduced to approximately 87.8%, while at 3,100 μm and 4,000 μm, it decreases to 50.0% and 33.3%, respectively. For the extreme case of 10,000 μm, efficiency is approximately 11.1%. Figure 8 illustrates this trend clearly, showing a plateau at 100% efficiency up to approximately 2,000 μm, followed by a monotonic decline with increasing droplet diameter.

This result demonstrates that, under the selected containment geometry and spray fall height (100 ft), droplet diameters up to approximately 2,000 μm are sufficient to achieve near-complete thermal equilibration with the containment atmosphere. Above this threshold, residence time becomes insufficient for full heat and mass exchange, and the mechanistic CAP formulation captures this degradation without imposing a priori efficiency assumption.

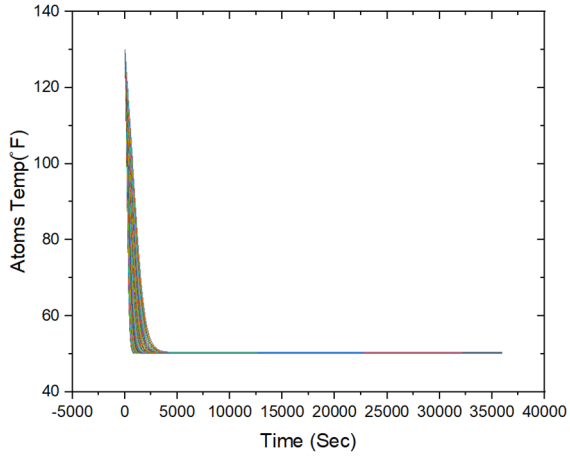


Fig. 3. Transient Response of Containment Atmosphere Temperature

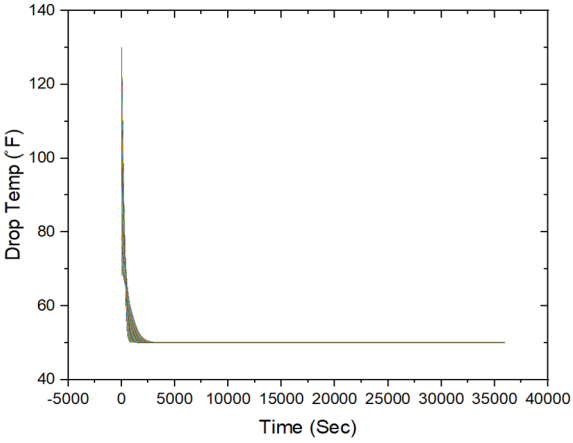


Fig. 4. Transient Response of Droplet Temperature

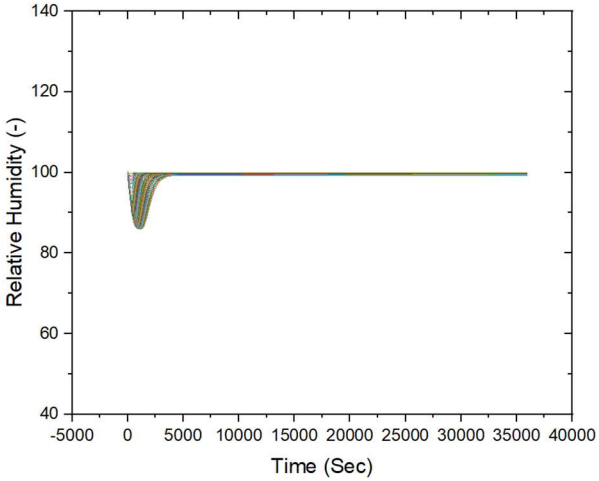


Fig. 5. Transient Response of Relative Humidity

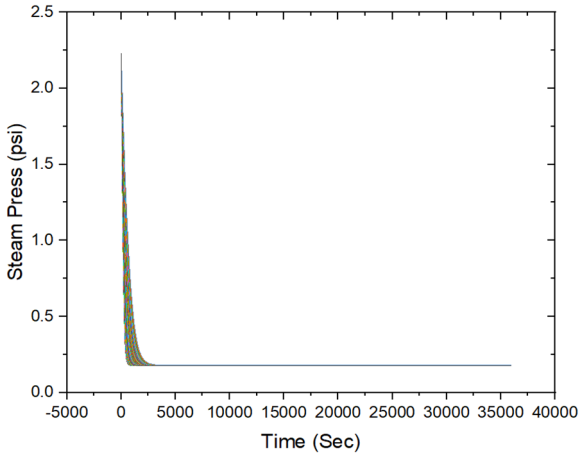


Fig 6. Transient Response of Steam Pressure

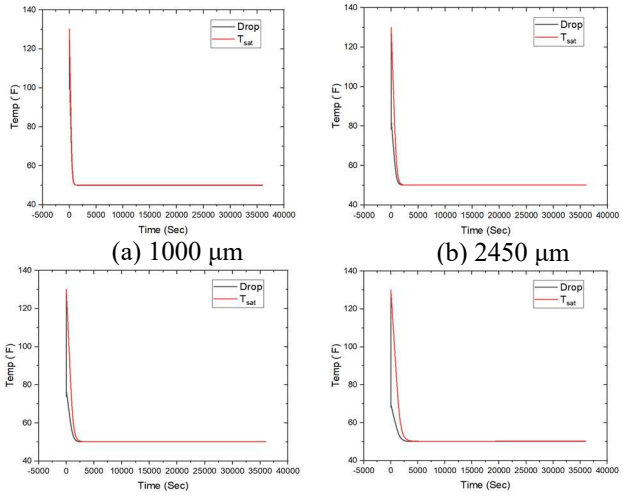


(a) 1000 μm (b) 2450 μm

(c) 3000 μm (d) 4000 μm

Fig. 7. Comparison of Saturation Temperature and Droplet Temperature

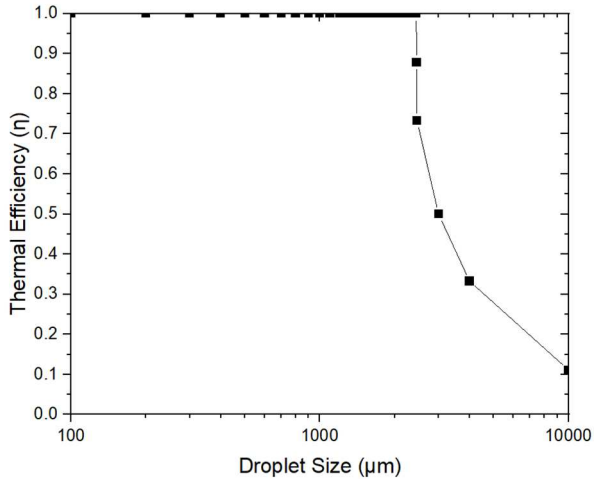


Fig. 8. Spray Thermal Effectiveness as a Function of Droplet Diameter

## 4. Conclusions

This study presents a mechanistic evaluation of containment spray thermal effectiveness using the CAP 3.1 three-field thermal–hydraulic model. Unlike conventional equilibrium-based approaches that require user-specified spray efficiency, the present methodology directly computes droplet–gas interfacial heat and mass transfer as a function of droplet diameter and residence height.

A structured parametric analysis was performed for droplet diameters ranging from 100 μm to 10,000 μm under a single-cell containment configuration representative of APR containment conditions. The droplet size spectrum was discretized consistently with ANSI/ANS-56.5 guidance, and steady-state spray thermal effectiveness was evaluated for each case.

The results show that spray thermal efficiency remains at 100% for droplet diameters up to approximately 2,000 μm under the assumed 100 ft fall height and specified thermodynamic conditions. Beyond this diameter, efficiency decreases progressively due to incomplete thermal equililibration between the droplet and the containment atmosphere. For very large droplets (10,000 μm), efficiency is significantly reduced, highlighting the importance of droplet size characterization in spray performance assessment.

The CAP-based mechanistic model provides a transparent and regulatorily defensible framework for linking nozzle droplet size distribution to credited spray thermal performance in containment P/T analysis. The methodology eliminates the need for purely assumed efficiency values and enables sensitivity-based justification of bounding spray parameters for licensing applications.

## REFERENCES

[1] “Development of APR NPPs’ Containment Pressure and Temperature Analysis Methodology using CAP Computer Code,” Journal of Mechanical Science and Technology (JMST).
[2] ANSI/ANS-56.5-1979, “American National Standard for PWR and BWR Containment Spray System Design Criteria,” Nov. 7, 1979.
[3] ANSI/ANS-56.4-1983 (R1988), Pressure and Temperature Transient Analysis for Light Water Reactor Containments, American Nuclear Society, 1988.
[4] S.-h. Jee et al., “Development of advanced containment thermal-hydraulic analysis methodology based on three-field model codes for APR1400,” Nuclear Engineering and Technology, vol. 57, art. no. 103616, 2025.
[5] W. E. Ranz and W. R. Marshall, “Evaporation from drops,” Chemical Engineering Progress, vol. 48, pp. 141–146, 1952.
[6] D. L. Brown, Vapor Condensation on Turbulent Liquid, Ph.D. dissertation, Massachusetts Institute of Technology, 1991.